Schumann resonance modes and ionosphere parameters: An annual variability comparison

Carlos Cano Domingo, Nuria Novas Castellano, Ruxandra Stoean, Manuel Fernandez Ros and José A. Gázquez Parra *Senior Member, IEEE*

***Abstract*—*Schumann Resonance* (SR) signals result from an electromagnetic wave that propagates along the Earth-Ionosphere cavity. This signal is mainly characterized by the amplitude and frequency of the first modes; however, the relation with other variables that affect the Earth-ionosphere cavity is still undiscovered. In this paper, this relation is further explored with a methodology based on the usage of the first six SR modes and focusing on separating the data by the hour of the day. In this research, SR data is cross-correlated with 14 variables that affect the Electromagnetic cavity. The result shows preliminary evidence about the relationship between SR data and ionospheric related variables such as the Virtual Height of each Ionospheric layer or Solar Flux. The research outcome also provides substantial support for the importance of aggregating all the information contained in the first six modes and also reinforces the previous evidence about the significance of separating the SR variation by 24 hours to avoid the masking effect produced by the daily variability. This work also gives new perspectives for predictors based on SR modes.**

***Index Terms*—Schumann Resonance modes, Earth-ionosphere cavity, Lightning discharge, ionospheric variables, natural correlation**

I. Introduction

SCHUMANN Resonances (SR) is the name given to the electromagnetic resonant phenomenon originated by the excitation of the earth ionosphere cavity [1], [2]. The earth-ionosphere wave guide cavity is formed by an insulator - the atmosphere - and two spherical media with a certain conductivity - the Earth's surface and the ionosphere's lower layer. The study of SR characterization has been widely addressed over the last 50 years. One common approach is to find models that match the experimental data recorded in different observatories over the world. [3], [4].

Other approaches are focused on establishing a possible link between SR variation and other natural phenomenon. It is broadly accepted that the main source of the cavity's excitation is the global lightning activity [5]. Therefore, one of the main subjects of study in the field of the SR has been the global thunderstorm centers, the name given to the three places on earth where lightning activity is highest at specific times of day [6]. The influence these thunderstorm centers have on SRs hourly activity has been preliminary demonstrated [7]. Recently, a most detailed study of the correlation has been published [8], but the nuances of this interaction are yet to be uncovered. Recently, a work uses the 1st mode to estimate the global lightning activity [5]. There is also a completely documented relation between these parameters, focused on the 1st mode [9]. In this book, the authors establish the highest lighting activity as [7:00 - 13:00], [14:00 - 17:00], [20:00 - 2:00] UTC Time Asian, African and American thunderstorm respectively.

Other studies have explored how SRs are influenced by the rest of environmental variables. One of the most popular examples is the relationship between the peak intensity of the fundamental mode of SR and global temperature, which was proposed by [10]. A growing interest has been developed for studying the effect of earthquake activity on SRs, looking for an indicative that allows early detection [11], [12].

Nonetheless, other studies have been focused on different natural events such as solar proton events [13], [14] or Gamma rays [15], even the seasonal and daily variations [16] of the SR signal itself.

It is also important to mention that the characterization gives useful insights about the variation of SR, especially in the frequencies values. These variations are mainly affected by meteorological factors, solar ionizing flux and solar wind condition [17], [18]. The most studied periodic variations of the ionosphere are driven by the same periodical phenomena on the earth-sun: 11-year solar cycle, 27-day rotation and day-night cycle. The orientation of the Earth with respect to the sun causes local variations as well, with the most remarkable ones being day night asymmetry and the seasonal asymmetry [19].

The Ministry of Economics and Competitiveness of Spain financed this work, under Project TEC2014-60132-P, in part by Innovation, Science and Enterprise, Andalusian Regional Government through the Electronics, Communications, and Telemedicine TIC019 Research Group of the University of Almeria, Spain and in part by the European Union FEDER Program and CIAMBITAL Group by I+D+I Project UAL18-TIC-A025-A, the University of Almeria, and the European Regional Development Fund (FEDER). We also thank the Andalusian Institute of Geophysics.and also the Proyecto-Puente2021-001, University of Almeria.

The authors will thanks the Global ionospheric radio observatory (GIRO) to provide measurement of virtual ionospheric layer height. https://hpde.io/SMWG/Observatory/GIRO.

NLDN data provided by the NASA Lightning Imaging Sensor (LIS) instrument team and the NASA LIS Data Center via the NASA EOSDIS Global Hydrology Resource Center (GHRC) DAAC located at the Global Hydrology and Climate Center (GHCC), Huntsville, Alabama through a license agreement with the Vaisala Group. The data available from the NASA EOSDIS GHRC DAAC are restricted to collaborators that have a working relationship with the NASA Marshall Space Flight Center (MSFC) Lightning Group.

R. Stoean was supported by a grant of the Romanian Ministry of Research and Innovation, CCCDI – UEFISCDI, project number 178PCE/2021, PN-III-P4-ID-PCE-2020-0788, within PNCDI III. Carlos Cano thanks the European Union's support and the Ceia3 for funding the mobility program.

Carlos Cano, Nuria Novas, Manuel Fernandez and Jose A. Gazquez are with the Department of Engineering, University of Almeria, Almería 04120, Spain (e-mail: carcandom@ual.es; nnovas@ual.es; mfernandez@ual.es; jgazquez@ual.es)

Ruxandra Stoean is with Romanian Institute of Science and Technology, Romania (e-mail: ruxandra.stoean@rist.ro)

The latter is actually two-fold. First, there are discrepancies between hemispheres for a given moment in time and second, there are differences for any given season on each hemisphere as well, produced by the sun being closer to the Earth during the northern hemisphere summer but farther away on the southern one [20]. These changes are still under study with the goal of finding an accurate predictor. New models have been proposed in order to improve the accuracy of the ionosphere variation prediction [21].

It is also important to mention the natural relation between the height of the ionosphere and lightning activity. Lightning activity is more intense when the ionosphere is very close to the earth, and it leads to a change in the ionosphere cavity [22].

Many studies have been carried out for understanding the relation between SRs frequency and condition of the lower ionosphere. In [23], the author explains the dependency of SR modes and the vertical profile of the ionosphere. In [24] the very low frequency (VLF) band is used to study the characteristics of the ionosphere due to the frequency dependency of the ionosphere conductivity. Another author [25] also uses the extremely low frequency (ELF) band to monitor the height of the D-layer. In this paper, the researchers use a reflection height dependent on the frequency.

It is possible to conclude that SR variability and ionospheric variables have been individually analyzed and also studied in regard to the SR relation with a particular ionosphere variable, with a very specific approach. However, to the best of our knowledge, there is only ongoing research with the focus on studying the interaction between multiple ionospheric variables and their relation with different SR modes. Exploiting all the data available will provide valuable insight in the study of SR. Please note that, although different variables are considered (e.g. Solar, Lightning etc), for convenience reasons, we will use the encompassing term *ionospheric* for referring to all of them.

There are two facts that give way for improvement and development of a methodology that may fulfill the requirements for this study.

First, due to the fact that the propagation characteristic in a complex cavity is highly dependent of the signal frequency, the information contained in each SR mode can have substantial differences. Although there are several studies about the relationship between SR and ionospheric variability [8], [13], [26], [27], most of them consider only the fundamental mode, missing the possible information that other SR modes provide.

Secondly, most studies have tended to focus on the relation between ionosphere long-term variability and SR variations by averaging daily values [6], [28]. Although this approach is entirely valid and has produced many valuable results, it suffers from the analysis of the long-term relation for specific hours, which are not masked by the day to day variability. It is also important to notice that since SR are partly defined by the ionospheric conductivity profile, ionospheric variations should be reflected in SR records. Nonetheless, when accounting all the parameters that usually define the conductivity profile of the ionosphere, a new approach is clearly needed, one that analyzes which variable is responsible for a specific behavior.

By taking into account all measurable modes and working with hourly averaged frequency for each one, its comparison with the most relevant parameters that affect the ionosphere composition would yield the mode and hour where each ionospheric parameter influences SR the most. Although SR response depends on the general state of the ionosphere, certain ionospherical parameters may be dominant at certain times of the day, for certain modes. Thus, by cross-correlating hourly averaged activity with ionospherical data, strong correlations may indicate which parameters are dominant at specific hours and over which SR modes. In other words, finding an hour in which the activity of a particular parameter of the ionosphere rules out the rest implies that there is no other relevant effect in the electromagnetic cavity that could obscure its impact in the SR frequency variation records. By tracking this hour along different years, it would be possible to see a similar pattern between this effect and the variability of the SR mode. As a base to test this hypothesis, this paper will investigate the relation between ionosphere parameters variability over the 5-year period from 2016 to 2020 in comparison with the first six modes of the SR during the same period of time.

II. Data and Methodology

The data used in this research along with a brief explanation about the proposed methodology is exposed in this section.

A. External Data

1) Solar Data

The number of sunspots has been obtained from [29]. The number of sunspots is an historical measurement related to the intensity of the Solar activity. Along the 11-year not only the number of sunspot varies but also they move from one hemisphere to the other. Specifically, at the beginning of the 11-year solar cycle the density of sunspot is higher in the northern hemisphere and moves to the southern hemisphere [30].

- **Sunspots (sunspot)**: Number of sunspots per day.
- **Northern Hemisphere Sunspots (sunspotN)**: Number of sunspots per day in the Northern hemisphere.
- **Southern Hemisphere Sunspots (sunspotS)**: Number of sunspots per day in the Southern hemisphere.

Solar Flux [31] is the electromagnetic power received by the sun per surface unit measured in $1 \times 10^{-22}\,\mathrm{W}/(\mathrm{m}^2\,\mathrm{Hz})$:

- **Adjusted Solar Flux (SolarFlux)**: Standard method to estimate the real solar flux from the observable measurement of the magnetic flux received on the Earth's surface.

2) Ionospheric Data

Layer height from GYRO [32] - the values are the minimum virtual height [F/F2/E/Es] traces measured in km. A complete description about the ionosphere layer composition can be found in [33]:

- **Sporadic E Layer (hEs)**: The result of wind shears, meteors and other phenomena.
- **E Layer (hE)**: Particles ionized due to soft X-ray (1–10 nm) and UV.
- **F1 Layer (hF1)**: Strongly affected by the solar radiation.
- **F2 Layer (hF2)**: Variations are usually large, irregular, and particularly pronounced during magnetic storms.

Total number of electrons in the D layer - simulation based on International Reference Ionosphere (IRI2016) [34]:

- **Simulated TEC in D layer (TEC-D)**: The data unit is in $1 \times 10^{-16}/\mathrm{m}^2$.

Number of electrons extracted from the database GYRO [32]:

- **Total Electron Content (TEC)** $1 \times 10^{-16}/\mathrm{m}^2$. Highly dependent of Solar Flux.

3) Earth Data

Geomagnetic indexes from [35]:

- **Geomagnetic Index Kp (Kp)**: The K-index is quasi-logarithmic local index of the 3-hourly range in magnetic activity relative to an assumed quiet-day curve for a single geomagnetic observatory site.
- **Geomagnetic index Ap (Ap)**: The Ap-index is defined as the earliest occurring maximum 24-hour value obtained by computing an 8-point running average of successive 3-hour Ap indices during a geomagnetic storm event, and is uniquely associated with the storm event.

Total number of Lighting strikes measured in the US [36]:

- **Lightning Activity (Lightning)**: Strikes per day.

Temperature obtained using the database in [37] using the last improvements, as explained in [38]:

- **Global Temperature (Temp)**: Global temperature anomaly measured in degrees.

B. Schumann Resonance Data

SR data has been recorded continuously since 2015 at the Sierra de Filabres observatory in Almería, Spain. A picture of the observatory can be seen in Fig. 1.

Fig. 1. Sierra de los Filabres ELF observatory.

The observatory is composed by two high precision sensors with a frequency response able to capture the SR signal up to 100 Hz. The digitalizer is composed by a 24 bit ADC and a sampler rate of 187 samples per second. A photo of the observatory and sensors. The data is captured in 30-minutes registers by two perpendicular sensors, one oriented North-South and the other East-West. Each file is processed using a transform to the frequency domain, and a fit to a sum of Lorentzian functions. After the fitting process, the extraction of the peak frequency and intensity for each mode is obtained.

An example of a 30-minutes segment can be seen in Fig. 2. The Lorentzian curve fit to the data is represented by a blue line along with the six vertical lines for each of the SR modes. It is possible to see that even with a low signal level for the last two modes, the methodology implemented can extract an accurate value of the central frequency for the first six modes. Contrary to most of the SR observatories, we have preserved the information up to the 6th SR mode because, on preliminary studies of our data, we have observed a different behavior of the last two modes compared to the others. Then these SR modes can provide helpful information about the SR-ionosphere relationship. A more detailed explanation of the process and the day-to-day variability can be found in [16] for the years 2016 and 2017.

In the present work, the results are obtained from 1st January 2016 to 31st December 2020.

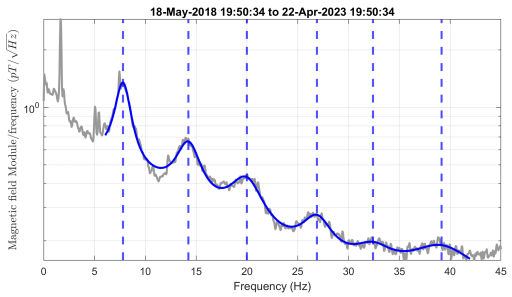

Fig. 2. An example of a Schumann Resonance spectrum taken in the Sierra de los Filabres ELF observatory. Gray curve: Raw SR signal; Blue curve: Lorentzian fit; Blue vertical lines: frequency value of each SR mode.

C. Methodology

The present study is focused on tracking changes in the ionosphere by means of the SR frequency variations, in $Hertz$, in a way where the most number of variables can be accounted for. As advanced in Section I, this analysis is based on the hypothesis that the ionospherical parameter that affects one or more SR modes the most changes over time. Consequently, by extracting the hourly averaged peak frequency, in $Hertz$, for each of the first six modes and grouping them by the hour of the day, we could verify through cross-correlation at which hour a specific mode shows the same tendency as a certain ionospheric parameter.

To implement the idea above and shape the analysis, data has been preprocessed as follows:

1) Data is divided by hours, and the frequency spectrum of each segment is extracted from the SR records.
2) Each of the produced frequency registers contains the hourly average peak frequency of each mode up to the sixth. From each month and each mode, the values above are further averaged, producing 24 hourly averaged peak frequency by month for each mode.
3) The ionosphere parameters described above are treated to homogenize them.

From there, each data set produced for each hour and each mode is cross-correlated with every data set from the parameters of the ionosphere. The Pearson correlation coefficient (r), using Eq. 1 gives us an indication on how closely the measured peak frequency on that hour follows the

ionospherical parameter's variations, where x and y represent the two variables under study.

$$r = \frac{\sum_{i=1}^{n}(x_i - \bar{x})(y_i - \bar{y})}{\sqrt{\sum_{i=1}^{n}(x_i - \bar{x})^2}\sqrt{\sum_{i=1}^{n}(y_i - \bar{y})^2}} \quad (1)$$

An example of this process can be seen on Fig. 3. The data depicted in Fig. 3a obtained a high and negative correlation value. Fig. 3b showed a low correlation value. For each correlation, a student's T test is performed to assess its viability. The results of this test are considered along with the correlation coefficients to determine the validity of the results.

This study is performed on data from the period from 2016 to 2020, having full data registers for both the SRs and the ionosphere parameters. Given the above, this means 24 peak values for each 60 months for each of the first six modes of the SR for the NS mode and Frequency variation value, leading to a total of 24 hours $\times$ 6 modes data sets of 60 months.

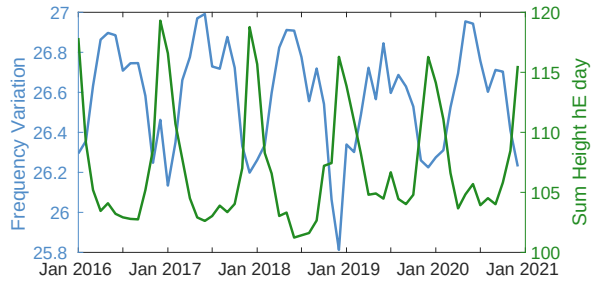

(a)

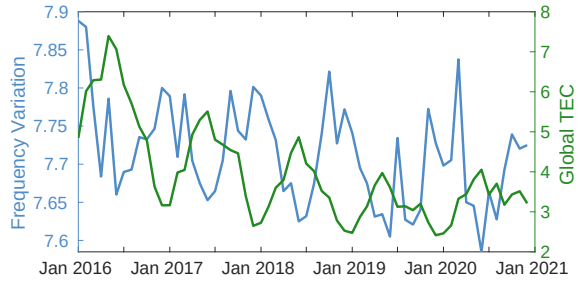

(b)

Fig. 3. 5-years time comparison between the Ionosphere parameters and SR mode frequency variation. (a) SR mode 4 at 11:00 and E layer Height. $r = -0.8, p = 10^{-13.9}$, (b) SR mode 1 at 11:00 and Total Electron Count. $r = 0, p = 1$.

III. Results

In this section, we present the results obtained by correlating the ionosphere variables under study with the data obtained in our observatory. The hours expressed in the results all refer to the UTC timezone. We have focused on the North-South sensor and the frequency variation mainly for two reasons. First, frequency variation is quite dependent on the conductive properties of the electromagnetic cavity on a given moment, so analyzing a single channel is enough to test the methodology, which is the goal of this article. Second, analyzing both channels would duplicate the amount of information to show, and given the high amount of variables involved in this work, we consider it would dilute the results more than reinforce them. Therefore, we have chosen to limit the presented result to the N-S channel.

A. Total relevant hours

Table I summarizes the results of the cross-correlation between SR modes and ionosphere parameters. There are two values for each mode and ionosphere parameter; total number of hours for which the Pearson correlation p-value is under 0.01 (left) and the averaged Pearson correlation coefficient for those hours (right). If no hour had a significant p-value for a given mode and parameter, the cell is left blank. A maximum p-value of 0.01 has been selected to ensure the statistical significance of this relationship. It can be established that there is only a 1% probability that the specific SR mode at the specific hour has no relationship with the ionospheric variable. Due to the constant value of the number of samples, 60, the Pearson correlation is completely related to the p-value. A $p - value < 0.01$ implies a Pearson correlation of at least 38%.

The height parameters will be presented next. The lower layer of the ionosphere - **D layer** - has an important factor of correlation with the 2nd, 3rd and 4th mode. The next **E and Es layers** display a similar behavior, but less related to the second mode and more with the 4th and 5th modes. **F layer** breaks the pattern above, with the highest number of hours belonging to the 1st mode and showing no relationship with the 6th. On the contrary, **F2 Layer** has the highest number of hours on which the correlation is significant, and higher correlation coefficients than the rest of layers. This is surprising since this layer is mostly relevant during the night hours. It is also the layer better correlated with the 5th and 6th modes.

TABLE I
SUM OF TOTAL HOUR WITH A CORRELATION -VALUE LOWER THAN 0.01, (H): NUMBER OF HOURS, (%): MEAN CORRELATION.

	Mode 1		Mode 2		Mode 3		Mode 4		Mode 5		Mode 6	
	H	%	H	%	H	%	H	%	H	%	H	%
hD	9	42	16	58	20	65	16	62	13	49	11	53
hE	10	42	13	50	18	65	17	62	5	51	10	54
hEs	10	42	14	50	19	61	16	62	5	47	10	51
hF	14	41	8	52	11	40	8	40	4	36	2	36
hF2	14	45	17	59	20	67	17	64	13	56	10	58
TEC	11	43	10	54	14	56	13	51	3	42	9	40
sunspot	23	55	14	43	11	41	6	41			2	37
sunspotN	20	52	14	41	4	48	1	50			2	41
sunspotS	21	44	4	46	9	40	4	47	8	37		
Kp	21	59	6	48	2	44	4	43				
Ap	22	58	6	46	3	42	4	43	1	34		
Lightning	7	44	18	61	20	57	16	56	16	49	10	56
Temp					4	35	2	38	5	39	4	43
SolarFlux	19	52	11	41	8	42	5	43			1	34

Regarding **TEC**, the relation with almost all modes is clear, showing significant correlations for an average of 11 hours, except with this 5th mode on which it only correlates for 3 hours, and with not a too high value of correlation. For the rest of SR modes, the mode with the most significant correlations is the 3rd, with 14 hours, and the one with the less is the 6th with 9.

Sunspot values (both total - **sunspot** - and separated by hemisphere - **sunspotN** and **sunspotS**) show a clear correlation with the first mode, in which almost all hours of the day are significant. The presence of this dependency decreases in

the higher SR modes, with only 6 hours showing a significant correlation in the 4th mode and absent in the 5th. Although two hours correlated significantly with the 6th mode, the correlation coefficient is very low. Northern sunspots display a correlation with the 2nd mode similar to the one of global sunspots, whereas the southerns are only significant during four hours. That being said, southern sunspots have more hours for the rest of modes than the northern, showing similarities in tendency even with the 5th mode, but once again with a low correlation coefficient.

The geomagnetic indexes, **Kp** and **Ap**, seem to have a high influence over the 1st mode, with the highest average correlation coefficient for this mode and all hours of the day except two being significant. However, this relation is not observable for the rest of modes. Both indexes display a very similar behavior, which is to be expected given the way **Ap** index is directly derived from **Kp**.

The daily mean of **Lightning** discharges displays a strong relationship with the 2nd, 3rd, 4th and 5th mode. The relation is also relevant for the 6th mode. Contrary to the rest of the parameters, the lowest average correlation coefficient of this variable belongs to the 1st mode. The number of significant hours is also lower on this mode than on the rest.

Global temperature (**Temp**) is not very relevant for any of the SR modes, especially for the first two modes, in which no hour displays a correlation whose significance goes above the specified threshold. Although this result may result surprising and against the accepted literature [10], it is important to remark that the relation under study is focused on frequency variations, while most of the previous studies that explored the relation between global temperature and SR are centered in the intensity variations of the latter.

Solar magnetic Flux (**SolarFlux**) correlates significantly with the 1st mode for 19 hours of the day, with an average correlation coefficient of 52% which is worthy of attention. The number of significant hours for the rest of modes is considerably lower, decreasing as the mode order increases and disappearing in the 5th mode. Average correlation coefficients for these modes are also lower than the one obtained for the 1st but consistent, being around 42%.

B. Hour Correlation

The results are summarized in a set of heat maps. Each heat map is composed by the values of the correlation between the ionospheric variable under study and the evolution of the SR mode at a specific hour. Each column represents a particular SR mode, while the rows are for the hour of the day of the selected SR mode. Colors express the intensity of the correlation as well as the sign. Red colours are for a high positive correlation and blue colours for the negative one. As expected, different patterns emerge from the correlation between SR peak frequency modes by hours and the evolution of each ionosphere parameter, which provides considerable insight into the relationship between them. However, this analysis offers preliminary evidence for the relation between a specific time interval of the SR mode with a particular parameter of the ionosphere. In the following, the relation between each mode and the ionosphere parameters will be studied in depth.

1) Ionosphere Virtual Height. The patterns mentioned above can be clearly observed in Fig. 4, where the most relevant hours shift for each mode and layer, but with an observable relationship between them. It can be observed that the **E and Es layers** layers have an almost completely identical pattern. The 1st mode is positively correlated at 11:00 and negative at 6:00. However, this correlation is far lower than with the rest of the mode. It can be seen that a negative correlation expands around 12:00 in the higher modes, starting with an interval of 2 hours in the 2nd mode, 6 hours in the 3rd mode and 8 hours in the 4th mode. Surprisingly, in the 5th mode it is not possible to see this pattern while the 6th mode returns to this behavior.

The next layer, **F layer**, shows an important positive correlation for the hours between 23:00 and 6:00 in the 1st mode, whereas the 2nd mode mirrors the 1st, having its peak correlation value when the 1st mode is at its lowest and vice versa. For the rest of the hours and SR modes, there is not a clear tendency. For the **F2 layer**, the same behavior is clear as for the **E and Es layers**, however it is inverted. To expose the differences between these layers, during the interval from 8:00 to 15:00, the **F2 layer** shows a higher intensity of the correlation and the number of hours with this correlation than the **E and Es layers**. In the same way, the negative correlation appearing in the **F layer** for the hours 22:00 to 2:00 in the 2nd and 3rd mode appears as positive in the **E and Es layers**.

2) Ionosphere Electron Content D layer. The lowest layer of the ionosphere, **D layer**, is not continuously measured and the simulation has to be performed to obtain the time variation characteristic. The correlation between the simulated electron content of the **D layer** and the hourly SR frequency mode variation is shown in Fig. 5. Unexpectedly, the results of this layer are very close to the result for the **F2 layer**, although there is a large difference in distance between them.

Apart from that, there are minor differences in the intensity of some hours. For example, in the SR mode 1:00 at 6:00, the correlation value is significantly higher for this layer than the F2. The higher values of F2 with the 3rd mode are also noticeable. One of the most striking results to emerge from the data related to the Ionosphere layers is that the correlation is far more intense during the central hours - 10:00 to 16:00 - just for the upper SR mode, specifically for the 3rd and 4th modes, and not with the 1st mode. This aspect will be discussed in detail in the discussion section.

3) Total Lighting Discharges. In Fig. 6, the correlation can be observed. For the 1st mode, the values are considerably lower than for the rest of the modes. In 2nd mode, there are three main intervals with very high values, two with a negative correlation: from 22:00 to 4:00 and from 16:00 to 18:00, and one with positive: from 11:00 to 12:00. The most striking part is related to the interval between 16:00 and 18:00, this correlation is neither present in any other mode nor for other ionosphere variable. For the rest of the SR modes, the pattern is very similar to the previous comment for the **D layer**, except lower correlation values during the central hours, and higher during the night hours. It is also important to notice the high

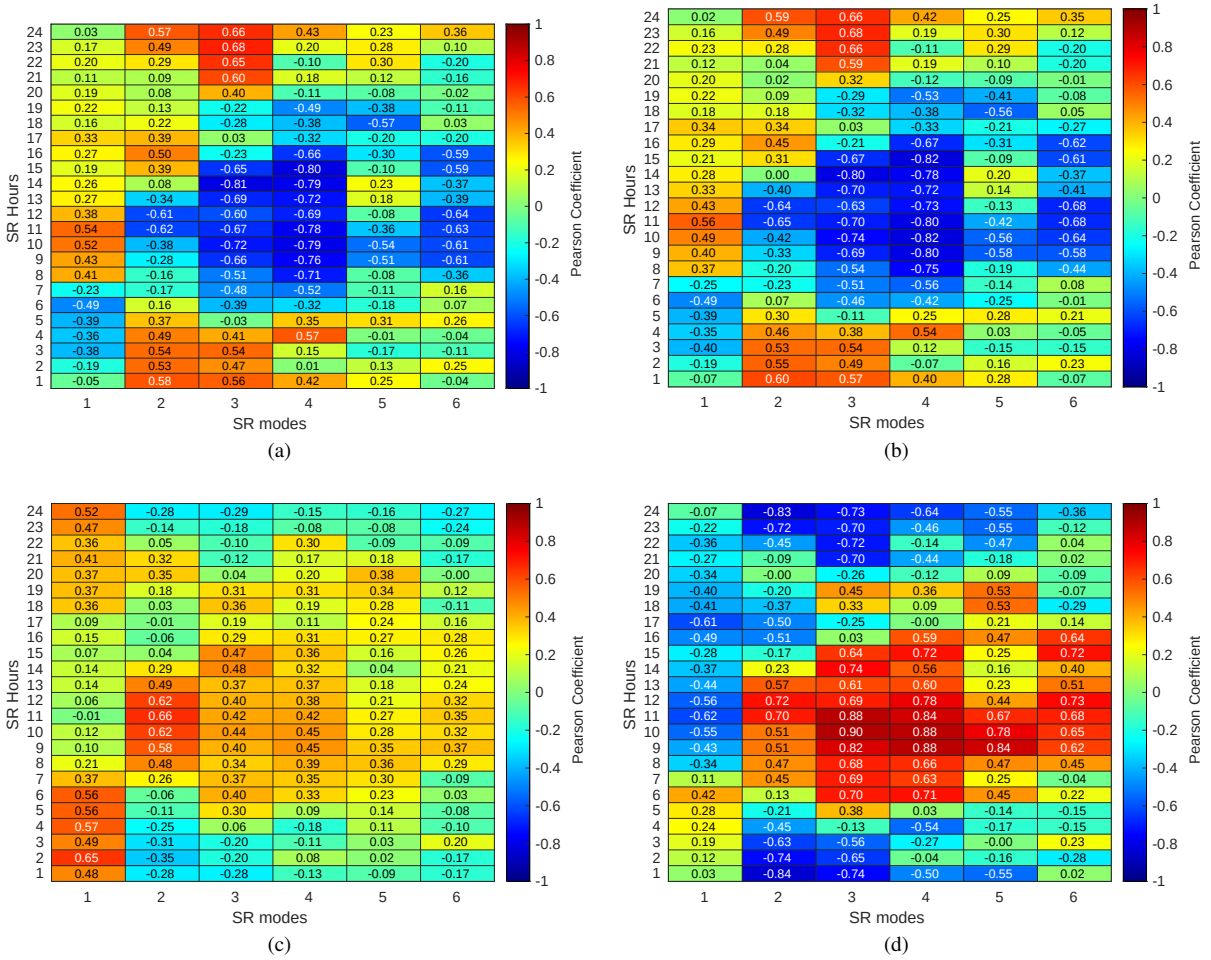

Fig. 4. Pearson Correlation coefficient between SR modes and ionosphere Height measurement, separated by hours. The Y-axis represents the time interval selected for the SR peak frequency mode. The X-axis represents the SR mode selected. (a) Virtual Height of The Sporadic E ionosphere Layer, (b) Virtual Height of The E ionosphere Layer, (c) Virtual Height of The F ionosphere Layer, (d) Virtual Height of the Sporadic F2 ionosphere Layer.

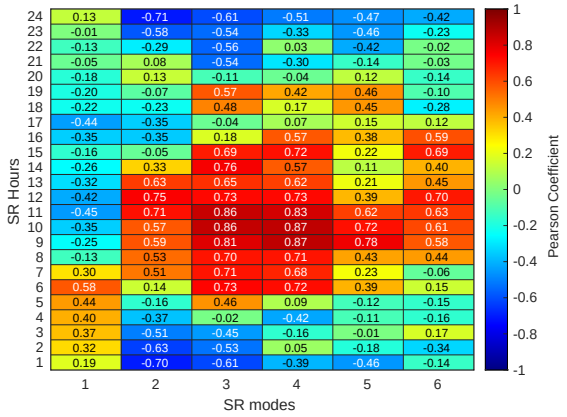

Fig. 5. Pearson Correlation coefficient between SR modes and Number of Electrons in D layer, separated by hours. The Y-axis represents the time interval selected for the SR peak frequency mode. The X-axis represents the SR mode selected.

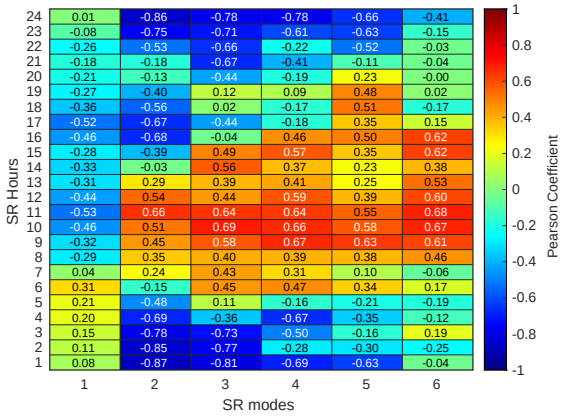

Fig. 6. Pearson Correlation coefficient between SR modes and Lightning Discharges, separated by hours. The Y-axis represents the time interval selected for the SR peak frequency mode. The X-axis represents the SR mode selected.

value of the 6thth modes during central hours, higher than in the previously commented ionosphere variables.

4) Global Temperature Anomaly. Unlike other research carried out in the area, we did not find a significant relation between global temperature anomaly and SR modes frequency variation. The low values of the correlation can be seen in Fig. 7. The highest values of correlation appear in the 3rd mode, for 5 hours, and with not a very relevant value of 40%,

approximately.

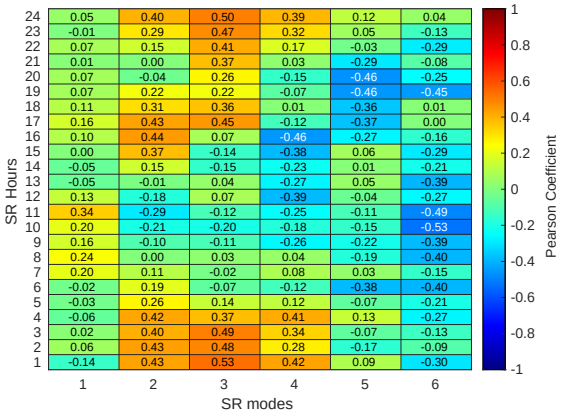

Fig. 7. Pearson Correlation coefficient between SR modes and Temperature anomaly, separated by hours. The Y-axis represents the time interval selected for the SR peak frequency mode. The X-axis represents the SR mode selected.

5) Solar Magnetic Flux and Total Electron Content. In Fig. 8, the estimate magnetic flux from the sun and the **TEC** can be seen. These two ionospheric variables show a strong relation for the 1st mode.

In the case of the Solar Flux, this relation lasts from 18:00 to 7:00, while for the **TEC** it is shorter, from 2:00 to 6:00. For the rest of the modes, there is not high correlation for the Solar Flux, except at 22:00 in the 4th mode. However, the **TEC** exposes a total different behavior, with a very strong relation for the 2nd, 3rd and 4th modes. It is also interesting that high values are obtained between 18:00 and 19:00 for the 3rd mode. All the correlations with these two variables are just positive.

6) Geomagnetic Index and Total Number of sunspots. In Fig. 9, the relation between the geometric index and total sunspot can be seen. The geometric index **Kp** and the hemispheres sunspot have been omitted because it shows the same pattern in these graphs compared to the respective ionosphere variables. The results show a very important relation between these two ionosphere variables and the 1st mode, with a high value of correlation which lasts around 12 hours for the geometric index **Ap** and 16 hours for sunspot. It is also important to notice two intervals in the sunspot case: for the 3rd mode, there is a high value at 18:00 and another in the 4th mode at 22:00. There are not clear correlations with the rest of the modes.

All the previously commented figures have been summarized in Table II. This table exposed the most correlated intervals for each parameter and for the six first modes. In this table, the maximum p-value is 0.001. Therefore, the values of the correlation are considerable higher than in the previous table. The result shows a clear pattern between SR modes and ionospheric parameter groups. Table III shows for each external variable the SR mode with the highest mean correlation. Only the values with a lower p-value than 0.001 have been considered. Considering the Ionospheric layers, three different patterns can be observed. First, **D**, **E** anb **Es** behave very similar, with SR mode 4th as the most important

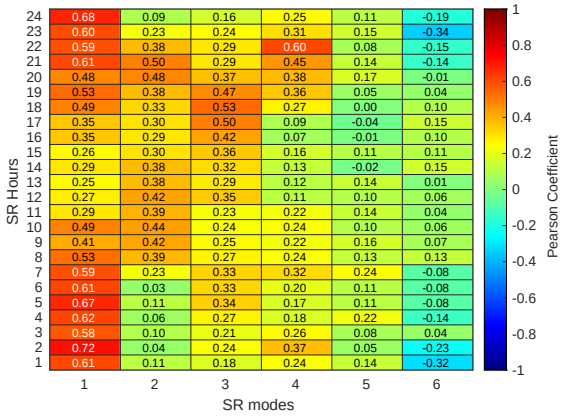

(a)

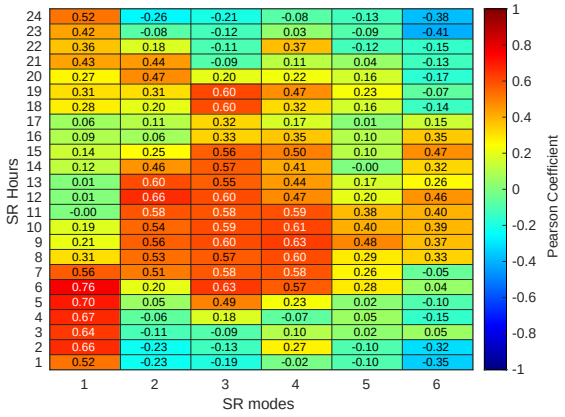

(b)

Fig. 8. Pearson Correlation coefficient between SR modes and (a) Solar Flux Adjusted, (b) Estimate Total Electron count, separated by hours. The Y-axis represents the time interval selected for the SR peak frequency mode. The X-axis represents the SR mode selected.

mode and a mean correlation value of 67%. Secondly, the hF2 mean correlation is also very high, around 70% for the selected hour, but with the 3rd SR mode. Finally, the hF differs completely with a mean correlation substantially lower than the other Ionospheric Virtual Layers and the 2nd as the most important. Solar Data shows a very similar pattern with the SR mode 1 as the most important and a value around 60%. As it was described previously, the Lightning data is highly related to the second SR, with a considerably high mean correlation of 48%. The temperature value is not very linked to any SR mode in terms of frequency variation. However, a higher correlation value can be observed in the SR mode 3.

IV. Discussion

The relation between some of the most relevant ionosphere parameters and the SR frequency peak variation has been studied. This result offers valuable insight into the relation between SR modes and specific ionosphere parameters. This underlines just how important is the SR mode in relation with the ionosphere. It is clear that not all Ionosphere parameters relate in the same way with each SR mode.

Even though the results related to the temperature obtained in this paper differ from previous studies [10], they provide valuable information. The relation with the first mode is not

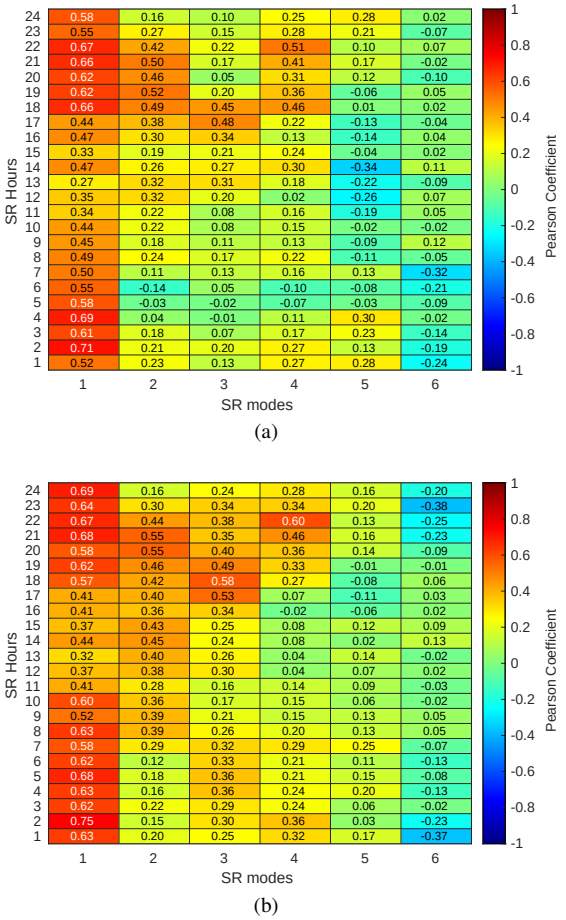

Fig. 9. Pearson Correlation coefficient between SR modes and (a) **Ap** geometric index, (b) Sunpots count in both hemispheres, separated by hours. The Y-axis represents the time interval selected for the SR peak frequency mode. The X-axis represents the SR mode selected.

the expected, while the relation with the higher modes is clearly satisfactory with previous evidences [9]. There are clearly 3 intervals, one positive from 16:00 to 20:00, which is similar to the African thunderstorm, another from 21:00 to 3:00 that is very close to the American thunderstorm and the third, positive, from 10:00 to 12:00, matching with the Asian thunderstorm center. These three correlation values in these intervals are very high during the 2nd mode. In the SR mode 6, the interval of the African thunderstorm disappears, the American one is not present, while the American one increases the value and the number of hours.

As stated at the start of this section, a strong relationship between the 1st mode and the lightning activity was to be expected [6]. Despite having significant correlation values at some hours, these are not as clear as those shown in the rest of modes. In line with the initial hypothesis of this work, the lessened correlation of the 1st mode with the lightning activity is pointing out how frequency variations in this mode are far more sensitive to changes in other parameters, for example the solar flux.

The virtual height of the ionosphere is a characteristic which summarizes the electron content of this layer [5]. From a theoretical point of view, when the ionosphere layer has a lower value, the cavity reduces their boundary condition so the

TABLE II
MAJOR CORRELATION INTERVALS WITH MEAN VALUE IN % FOR THE IONOSPHERE VARIABLES UNDER STUDIES FOR EACH OF THE FIRST SIX SCHUMANN RESONANCE MODES.

	Mode 1		Mode 2		Mode 3		Mode 4		Mode 5		Mode 6	
	H	%	H	%	H	%	H	%	H	%	H	%
hD	5- 7 11-13 17-18	51 -43 -44	7-14 23- 4	61 -65	5-16 18-20 21- 4	72 53 -56	4- 5 6-17 19-20 24- 1	-42 72 42 -51	8-12 18-20 22- 2	64 45 -45	8-14 15-17 24- 1	57 64 -42
hF	23- 7	50	8-14	58	10-12 14-16	43 48	9-12	44				
hF2	6- 7 9-14 16-19	42 -52 -50	7-14 16-18 22- 5	56 -50 -67	6-16 19-20 21- 4	73 45 -71	4- 5 6-17 21-22 23- 2	-54 71 -44 -55	6- 7 8-13 16-17 18-20 22- 2	45 64 47 53 -52	8-14 15-17	61 68
hE	6- 7 10-13	-49 49	10-13 16-17 23- 5	-57 45 54	6-16 21- 4	-64 65	4- 5 6-17 19-20 24- 1	54 -72 -53 42	9-12 18-19	-52 -56	8-13 15-17	-60 -61
hEs	6- 7 9-12	-49 50	11-13 16-17 23- 5	-62 50 53	7-16 21- 4	-64 65	4- 5 7-17 19-20 24- 2	57 -72 -49 43	9-11 18-19	-52 -57	9-13 15-17	-62 -59
TEC	21-22 23- 8	43 47	7-15 20-22	55 46	5-16 18-20	58 60	6-14 15-16 19-20	56 50 47	9-10	48	12-13 15-16	46 47
Sunspot	14-15 18-11	44 64	14-16 18-23	44 48	17-20	53	21-23	53				
SunspotN	18-11	56	8- 9 13-16 19-22	42 45 47	17-20	53	22-23	50			1- 2	-44
SunspotS	5- 6 8-11 19-20 21- 3	44 49 49 55	21-23	50	20-23	46	20-23	51	23- 0	41		
Kp	14-15 16-11	48 59	18-23	50	17-19	44	18-19 22-23	44 52				
Ap	14-15 16-11	47 59	18-23	48	17-19	46	18-19 22-23	46 51				
Lightning	10-13 16-18	-48 -49	9-13 16-19 22- 6	54 -64 -71	6- 8 9-13 14-16 17-18 20- 4	44 59 53 -44 -65	3- 5 6- 7 9-14 15-17 23- 2	-59 47 59 52 -70	9-12 16-17 18-20 22- 2	59 50 50 -61	8-14 15-17	59 62
Temp			1- 3 4- 5 16-18	43 42 43	17-18 23- 4	45 49	1- 2 16-17	42 -46	19-21	-46	10-12 19-20	-51 -45
SolarFlux	10-11 18- 9	49 57	9-11 12-13 20-22	43 42 49	16-20	48	21-23	53				

time to reach the whole cavity increases, then the frequency decreases. When the SR mode depends on a specific layer, it is expected to increase their frequency value when the height is lower.

The correlations shown in Section III are in good agreement with the studies previously mentioned. For the **E and Es layer**, the correlation is negative and near 70%. These layers are the lowest part of the ionosphere. It can be seen how 1st mode dependency with these layers is not quite strong, except at 6:00 and 11:00. These two hours are significant, since, by looking at other results, it is plainly clear that this SR mode has no other important correlation at these hours. This supports the grounds on which this work is based; at these hours, frequency variations on the 1st mode are mostly the result of the influences of the height on the **E and Es layers**. The close relation between the sixth modes and the lighting activity can be noticed in Fig. 10.

In the central hours, the correlation for almost all modes is negative, while at nighttime it is positive. It is important to mark that **E Layer** is mainly important during day hours.

TABLE III
IONOSPHERIC PARAMETERS BEST CORRELATION SR MODE

.

	SR Mode - Mean correlation
hD	SR Mode 4 - 67 %
hE	SR Mode 4 - 67 %
hEs	SR Mode 4 - 69 %
hF	SR Mode 2 - 58 %
hF2	SR Mode 3 - 70 %
TEC	SR Mode 3 - 59 %
sunspot	SR Mode 1 - 64 %
sunspotN	SR Mode 1 - 56 %
sunspotS	SR Mode 1 - 51%
Kp	SR Mode 1 - 57%
Ap	SR Mode 1 - 55%
Lightning	SR Mode 2 - 65%
Temp	SR Mode 3 - 48%
SolarFlux	SR Mode 1 - 56%

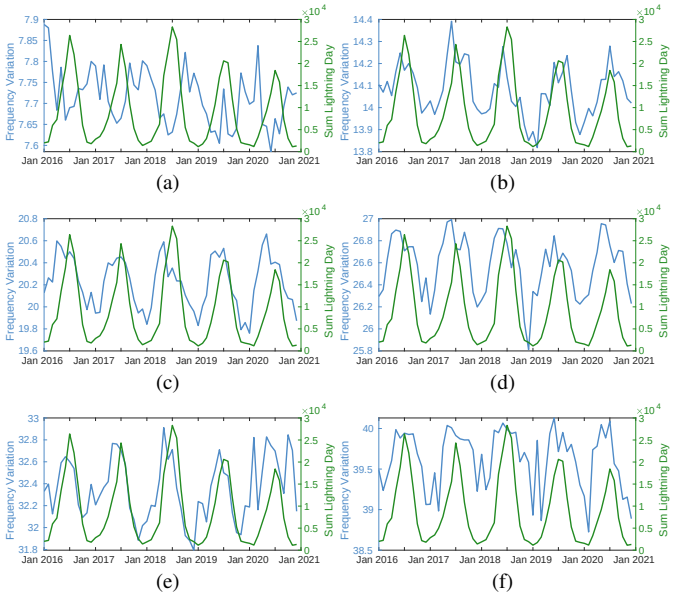

Fig. 10. Time evolution of the SR peak frequency mode at 11:00 and the total lightning discharges between 2016 and 2020. (a) 1st mode, (b) 2nd mode, (c) 3rd mode, (d) 4th mode, (e) 5th mode, (f) 6th mode.

However, due to the power line leakage in the 6th mode, the result of this mode presents a major source of unreliability. Contrary to expectations, **F2 layer** height and Electron content of the **D layer** behavior is the opposite of what was expected. It can be seen how, when the virtual height of this layer increases, the higher modes frequency also increases. In contrast, in the **F2 layer**, the 1st mode is very dependent on the relation previously mentioned. During the central hours, it can be established that the 1st mode has a boundary condition mostly related to the **F2 layer**. Therefore, observing **F layer**, during the nighttime the 1st mode is closely related to it. It can be explained by the asymmetries of the ionosphere around the globe. This relation is not present for the Electron content of the **D layer**, although it has a strong correlation at 6:00.

One of the most remarkable advances in SR studies was the link between SR and the Global Tropical Temperature by Williams et al. [10]. We have studied the relation between frequency variation and the temperature anomaly values. However, our results do not give a clear link between these two variables. It could be explained by the fact that our analysis is mainly focused on the frequency variation and finding a pattern which repeats over the 4 years, which is not the case of the global temperature. In the higher modes, it is possible to see some high values around midnight for the 2nd and 3rd modes.

The **Magnetic Solar Flux** is the main source of ionization for the ionosphere [33]. Nowadays, it is possible to monitor the solar flux, while historically this function was done by counting sunspots. In this paper, we have presented these three forms, i.e. Solar flux, Geometric index **Ap** and also sunspot. We can see that this parameter can be used to study the 1st mode. To the best of our knowledge, this relationship has not been exposed or theorized in the literature, and explaining it thoroughly is out of the scope of this article. Nonetheless, we can propose a couple of mechanisms that may explain it. SR energy is mainly focused on the first resonance due to the attenuation factor, which depends on SR mode frequency. These ionosphere parameters determine the baseline of the SR propagation and inject the energy for the lightning activity. That being said, further research is needed to characterize this relationship properly. It is also interesting to remark that the pattern shown in Fig. 8a and Fig. 9 is very similar and could be considered a demonstration of the common source of these three parameters. Solar Flux, Geomagnetic Index and Sunspot are all an expression of the Solar activity.

TEC is only important for the first mode during the interval from 0:00 to 7:00 and also during central hours for the 2nd, 3rd, 4th modes, due to the difference with other patterns, which need to be interpreted with attention in order to find a possible explanation.

V. CONCLUSIONS

To sum up, we have proposed a new approach for studying the relationship between some of the most important variables that affect the ionospheric and SR frequency variation for the first six modes. The methodology uses cross-correlation as the primary technique for analyzing the SR data from the Almeria Sierra de Filabres observatory (Spain) in the period from 2016 to 2020. Evidence from this study points out how these parameters affect over each SR mode changes hourly and hence provides valuable insight to the hypothesis of different ionospheric parameters being more relevant for different modes at different hours. We have obtained comprehensive results indicating that some SR modes are more sensitive to changes in particular variables, such as the Solar data with the SR mode 1 or the Ionospheric virtual Height Layers **D**, **Es**, and **E** with the SR mode 4. Although the correlation is not enough to establish a solid cause-and-effect relationship, these results provide a preliminary base for future work. This research opens new lines that could include the data from different observatories or a more complex mathematical or simulated model to establish a more reliable cause-effect relationship. The present findings might also suggest several courses of action to develop a computational model for predicting the variability of the earth's ionosphere using a combination of the frequency variability in different SR modes separated by the hour of the day.

REFERENCES

[1] W. O. Schumann, "Über die strahlungslosen Eigenschwingungen einer leitenden Kugel, die von einer Luftschicht und einer Ionosphärenhülle umgeben ist," *Zeitschrift fur Naturforschung - Section A Journal of Physical Sciences*, vol. 7, no. 2, pp. 149–154, 1952.

[2] T. Madden and W. Thompson, "Low frequency electromagnetic oscillations of the Earth-ionosphere cavity," *Reviews of Geophysics*, vol. 3, no. May, 1965. [Online]. Available: http://onlinelibrary.wiley.com/doi/10.1029/RG003i002p00211/full

[3] E. S. Goncharov, A. N. Lyakhov, and T. V. Loseva, "3D-FEM simulation model of the Earth-ionosphere cavity," *Journal of Electromagnetic Waves and Applications*, vol. 33, no. 6, pp. 734–742, 2019. [Online]. Available: https://doi.org/09205071.2019.1575289

[4] C. Kwisanga and C. J. Fourie, "3-D modeling of electromagnetic wave propagation in the uniform earth-ionosphere cavity using a commercial FDTD software package," *IEEE Transactions on Antennas and Propagation*, vol. 65, no. 6, pp. 3275–3278, 2017.

[5] E. Prácser, T. Bozóki, G. Sátori, E. Williams, A. Guha, and H. Yu, "Reconstruction of Global Lightning Activity Based on Schumann Resonance Measurements: Model Description and Synthetic Tests," *Radio Science*, vol. 54, no. 3, pp. 254–267, 2019.

[6] A. V. Koloskov, A. P. Nickolaenko, Y. M. Yampolsky, C. Hall, and O. V. Budanov, "Variations of global thunderstorm activity derived from the long-term Schumann resonance monitoring in the Antarctic and in the Arctic," *Journal of Atmospheric and Solar-Terrestrial Physics*, vol. 201, no. February, p. 105231, 2020. [Online]. Available: https://doi.org/10.1016/j.jastp.2020.105231

[7] M. Soler-Ortiz, M. F. Ros, N. N. Castellano, and J. A. Parra, "A new way of analyzing the schumann resonances: A statistical approach," *IEEE Transactions on Instrumentation and Measurement*, vol. 70, 2021.

[8] G. Tatsis, A. Sakkas, V. Christofilakis, G. Baldoumas, S. K. Chronopoulos, A. K. Paschalidou, P. Kassomenos, I. Petrou, P. Kostarakis, C. Repapis, and V. Tritakis, "Correlation of local lightning activity with extra low frequency detector for schumann resonance measurements," *Science of the Total Environment*, vol. 787, 2021.

[9] A. Nickolaenko and M. Hayakawa, *Schumann resonance for tyros: Essentials of global electromagnetic resonance in the earth-ionosphere cavity*. Springer, Tokyo, 2014.

[10] E. R. Williams, "The schumann resonance: A global tropical thermometer," *Science*, 1992.

[11] K. Florios, I. Contopoulos, V. Christofilakis, G. Tatsis, S. Chronopoulos, C. Repapis, and V. Tritakis, "Pre-seismic Electromagnetic Perturbations in Two Earthquakes in Northern Greece," *Pure and Applied Geophysics*, vol. 177, no. 2, pp. 787–799, 2020.

[12] J. A. Gazquez, R. M. Garcia, N. N. Castellano, M. Fernandez-Ros, A. J. Perea-Moreno, and F. Manzano-Agugliaro, "Applied engineering using Schumann Resonance for earthquakes monitoring," *Applied Sciences (Switzerland)*, vol. 7, no. 11, 2017.

[13] M. Sanfui and D. Biswas, "First mode Schumann resonance frequency variation during a solar proton event," *Terrestrial, Atmospheric and Oceanic Sciences*, vol. 27, no. 2, pp. 253–259, 2016.

[14] I. G. Kudintseva, S. A. Nikolayenko, A. P. Nickolaenko, and M. Hayakawa, "Schumann resonance background signal synthesized in time," *Telecommunications and Radio Engineering (English translation of Elektrosvyaz and Radiotekhnika)*, vol. 76, no. 9, pp. 807–825, 2017.

[15] A. P. Nickolaenko, I. G. Kudintseva, O. Pechony, M. Hayakawa, Y. Hobara, and Y. T. Tanaka, "The effect of a gamma ray flare on schumann resonances," *Annales Geophysicae*, vol. 30, pp. 1321–1329, 2012.

[16] C. Cano-Domingo, M. Fernandez-Ros, N. Novas, and J. A. Gazquez, "Diurnal and seasonal results of the Schumann Resonance Observatory in Sierra de Filabres, Spain," *IEEE Transactions on Antennas and Propagation*, no. 1962, pp. 1–10, 2021.

[17] J. M. Forbes, S. E. Palo, and X. Zhang, "Variability of the ionosphere," *Journal of Atmospheric and Solar-Terrestrial Physics*, vol. 62, no. 8, pp. 685–693, 2000.

[18] T. Bozóki, G. Sátori, E. Williams, I. Mironova, P. Steinbach, E. C. Bland, A. Koloskov, Y. M. Yampolski, O. V. Budanov, M. Neska, A. K. Sinha, R. Rawat, M. Sato, C. D. Beggan, S. Toledo-Redondo, Y. Liu, and R. Boldi, "Solar cycle-modulated deformation of the earth–ionosphere cavity," *Frontiers in Earth Science*, vol. 9, 2021. [Online]. Available: https://www.frontiersin.org/article/10.3389/feart.2021.689127

[19] T. Dang, W. Wang, A. Burns, X. Dou, W. Wan, and J. Lei, "Simulations of the ionospheric annual asymmetry: Sun-Earth distance effect," *Journal of Geophysical Research: Space Physics*, vol. 122, no. 6, pp. 6727–6736, 2017.

[20] Y. Jin and C. Xiong, "Interhemispheric Asymmetry of Large-Scale Electron Density Gradients in the Polar Cap Ionosphere: UT and Seasonal Variations," *Journal of Geophysical Research: Space Physics*, vol. 125, no. 2, 2020.

[21] X. BIN and Y. LIU, "Improved model of ionosphere variability and study for long-term statistical characteristics," *Chinese Journal of Aeronautics*, vol. 34, no. 2, pp. 407–419, 2021. [Online]. Available: https://doi.org/10.1016/j.cja.2020.03.018

[22] M. Friedrich and M. Rapp, "News from the lower ionosphere: A review of recent developments," *Surveys in Geophysics*, vol. 30, pp. 525–559, 2009.

[23] A. P. Nickolaenko, Y. P. Galuk, and M. Hayakawa, "Vertical profile of atmospheric conductivity that matches Schumann resonance observations," *SpringerPlus*, vol. 5, no. 1, pp. 1–12, 2016.

[24] K. L. Koh, Z. Liu, and M. Füllekrug, "Lower Ionosphere Effects on Narrowband Very Low Frequency Transmission Propagation: Fast Variabilities and Frequency Dependence," *Radio Science*, vol. 53, no. 5, pp. 611–623, 2018.

[25] M. Füllekrug, A. C. Fraser-Smith, and K. Schlegel, "Global ionospheric D-layer height monitoring," *Europhysics Letters*, vol. 59, no. 4, pp. 626–632, 2002.

[26] A. Pizzuti, A. Bennett, and M. Füllekrug, "Long-term observations of schumann resonances at portishead (uk)," *Atmosphere*, vol. 13, 1 2022.

[27] P. S. Figueredo, B. M. Ortega, M. Pazos, D. R. Osorio, E. A. Mascote, V. M. Mendoza, and R. Garduño, "Schumann resonance anomalies possibly associated with large earthquakes in mexico," *Indian Journal of Physics*, vol. 95, pp. 1959–1966, 10 2021.

[28] X. Y. Ouyang, Z. Xiao, Y. Q. Hao, and D. H. Zhang, "Variability of schumann resonance parameters observed at low latitude stations in china," *Advances in Space Research*, vol. 56, pp. 1389–1399, 2015. [Online]. Available: http://dx.doi.org/10.1016/j.asr.2015.07.006

[29] F. Clette and L. Lefèvre, "The New Sunspot Number: Assembling All Corrections," *Solar Physics*, vol. 291, no. 9-10, pp. 2629–2651, 2016. [Online]. Available: http://dx.doi.org/10.1007/s11207-016-1014-y

[30] P. Poudel, N. Parajuli, A. Gautam, D. Sapkota, H. Adhikari, B. Adhikari, A. Silwal, S. P. Gautam, M. Karki, and R. K. Mishra, "Wavelet and cross-correlation analysis of relativistic electron flux with sunspot number, solar flux, and solar wind parameters," *Journal of Nepal Physical Society*, vol. 6, pp. 104–112, 12 2020.

[31] K. F. Tapping, "The 10.7 cm solar radio flux (F10.7)," *Space Weather*, vol. 11, no. 7, pp. 394–406, 2013.

[32] B. W. Reinisch and I. A. Galkin, "Global ionospheric radio observatory (GIRO)," *Earth, Planets and Space*, vol. 63, no. 4, pp. 377–381, 2011.

[33] K. Rawer, *Wave propagation in the ionosphere*. Springer Science & Business Media, 2013, vol. 5.

[34] D. Bilitza, "IRI the international standard for the ionosphere," *Advances in Radio Science*, vol. 16, pp. 1–11, 2018.

[35] J. Matzka, C. Stolle, Y. Yamazaki, O. Bronkalla, and A. Morschhauser, "The geomagnetic kp index and derived indices of geomagnetic activity," *Space Weather*, vol. 19, pp. 1–21, 2021.

[36] D. J. Cecil, D. E. Buechler, and R. J. Blakeslee, "Gridded lightning climatology from trmm-lis and otd: Dataset description," *Atmospheric Research*, vol. 135-136, pp. 404–414, 1 2014.

[37] NASA Goddard Institute for Space Studies, "2019: GISS Surface Temperature Analysis (GISTEMP), version 4," 2019. [Online]. Available: https://data.giss.nasa.gov/gistemp/

[38] N. J. Lenssen, G. A. Schmidt, J. E. Hansen, M. J. Menne, A. Persin, R. Ruedy, and D. Zyss, "Improvements in the GISTEMP Uncertainty Model," *Journal of Geophysical Research: Atmospheres*, vol. 124, no. 12, pp. 6307–6326, 2019.